Heat Mass Transfer (2007) 44:125–136
DOI 10.1007/s00231-006-0227-2

ORIGINAL

3D numerical simulation on fluid flow and heat transfer characteristics in multistage heat exchanger with slit fins

W. Q. Tao · Y. P. Cheng · T. S. Lee

Received: 21 November 2006 / Accepted: 21 December 2006 / Published online: 24 January 2007

Abstract In this paper, a numerical investigation is performed for three-stage heat exchangers with plain plate fins and slit fins respectively, with a three-dimensional laminar conjugated model. The tubes are arranged in a staggered way, and heat conduction in fins is considered. In order to save the computer resource and speed up the numerical simulation, the numerical modeling is carried out stage by stage. In order to avoid the large pressure drop penalty in enhancing heat transfer, a slit fin is presented with the strip arrangement of "front coarse and rear dense" along the flow direction. The numerical simulation shows that, compared to the plain plate fin heat exchanger, the increase in the heat transfer in the slit fin heat exchanger is higher than that of the pressure drop, which proves the excellent performance of this slit fin. The fluid flow and heat transfer performance along the stages is also provided.

List of symbols

A	Heat transfer area (m^2)
c_p	Specific heat at constant pressure (kJ kg^{-1} K^{-1})
D_e	Outer tube diameter (m)
f	Friction factor
h	Heat transfer coefficient (W m^{-2} K^{-1})
L	Fin depth in air flow direction (m)
ΔP	Pressure drop (Pa)
Re	Reynolds number
T	Temperature (K)
$\vec{U}$	Velocity vector
u	Velocity in x direction (m/s)
v	Velocity in y direction (m/s)
w	Velocity in z direction (m/s)

Greek symbols

λ	Thermal conductivity (W m^{-1} K^{-1})
μ	Dynamic viscosity (kg m^{-1} s^{-1})
ρ	Air density (kg m^{-3})
Γ	Diffusion coefficient, λ/c_p
θ	Local intersection angle (degree)
$\overline{\theta}$	Mean intersection angle (degree)

Subscripts

in	Inlet
m	Mean
max	Maximum
min	Minimum
out	Outlet
w	Wall

W. Q. Tao (✉)
State Key Laboratory of Multiphase Flow in Power Engineering, Xi'an Jiaotong University,
Xi'an 710049, China
e-mail: wqtao@mail.xjtu.edu.cn

Y. P. Cheng · T. S. Lee
Laboratory of Fluid Mechanics,
Department of Mechanical Engineering,
National University of Singapore, Singapore,
Singapore 119260

1 Introduction

Fin-and-tube heat exchangers are commonly used in the HVAC & R, automobiles and air cooling industries, etc. it is an effective way to reduce the air-side thermal resistance which often accounts for about 90% of the overall thermal resistance. In order to reach this goal, different new types of fins were developed, such as the wavy fin, the louvered fin and the slit fin. Experimental studies for these different types of fins have been extensively performed. Recent investigations [1, 2] show that slotted fin with protruding strips which are parallel to the base sheet has the better performance than the wavy fin and the louvered fin, hence it is widely adopted in engineering, especially in air conditioning and gas cooling industry.

This kind of fin geometry was first studied by Nakayama and Xu [3]; they reported that its heat transfer coefficient can be 78% higher than that of the plain fin at 3 m/s air velocity, then followed by Hiroaki et al. [4], and their results indicated that the heat exchanger with slotted fins can have a 1/3 smaller volume than that with plain fin. Recently, Wang et al. [5–7] conducted a comprehensive experimental investigation for two types of slit fins with different protruding directions, and the experimental correlations of the heat transfer and flow friction were also developed.

Besides the studies on the characteristics of the whole fins, there are some investigations focused on the strips on the slit fin. Yun and Lee [8] analyzed the effects of various design parameters on the heat transfer and pressure drop characteristics of the slit fin heat exchangers, and presented the optimum value for each parameter. Kang and Kim [9] experimentally studied the effect of strip location on the heat transfer and pressure drop, and found that the slit fin with all the strips mainly positioned in the rear part has the better performance than that of the slit fin with all the strips in the front part. Qu et al. [10] validated numerically such an interesting finding and explained it from the viewpoint of field synergy principle, which was firstly proposed by Guo et al. [11, 12] for parabolic fluid flow and heat transfer. Later Tao et al. [13, 14] extended this idea from parabolic flow to elliptic flow.

From the traditional viewpoint the reasons why the interrupted fin surface can enhance the heat transfer is attributed to the decrease in the thermal boundary layer near the wall and/or the increase of the disturbance in the fluid. However, the field synergy principle attributes all the reasons to the improvement of the synergy between the local velocity and temperature gradient.

Based on field synergy principle Cheng et al. [15] proposed a new slotted fin with strips on the fin surface abiding by the rule of ‘‘front coarse and rear dense’’ along the flow direction, the numerical results show that the *j* factor of the new fin is about 9% higher than the fin with all the same number of strips in the front part. One object of this paper is to investigate the performance of this slit fin in the multistage heat exchanger, meanwhile, analyze the results with the field synergy principle.

In the practical application, a heat exchanger with a single fin along the flow direction sometimes cannot satisfy the real requirement; therefore, more fins are arranged in the line along the flow direction, which constitutes the multistage heat exchanger. Though the computer with large memory and high speed has emerged, it is still very difficult to simulate the multistage heat exchanger with a three-dimensional model, because with the increasing large grid number, it will be more time-consuming and the discretized governing equations have a more difficult convergence procedure. In this paper a novel method is presented to make the numerical modeling on the multistage heat exchangers quickly and accurately.

In the following presentation, the physical model and numerical formulation for the problem studied will first be presented, followed by the detailed descriptions of the numerical treatment of the plain fin and slit fin in the computation, and then numerical results on multistage heat exchanger with slit fin will be provided. The whole heat transfer and friction performance of two multistage heat exchangers with plain fin and slit fin is compared, so is the performance along the stages. Then the reason why the slit fin can enhance the heat transfer is analyzed with the field synergy principle. Finally some conclusions will be drawn which can be helpful in simulating the multistage heat exchanger.

2 Physical model

A schematic diagram of a three-stage plain plate fin-and-tube heat exchanger is shown in Fig. 1. The slit fin surface is alike except that there are many pieces of strips on the fin surface. In every fin there are three rows of tubes which are arranged in a staggered way, and the tubes and fins are both made of copper. In the flow direction three stages of fins are arranged in line in order to satisfy the practical need. The hot air from the compressor flows through the three stages from the left to the right, and the cooling water flows in the tubes. The heat is transmitted from the air to the tube wall and the fin surfaces, then to the cooling water. The air is assumed to be incompressible with constant property in every stage. The heat transfer and the pressure drop characteristics of the air side are solved by the numerical modeling. Because of the relative high heat transfer coefficient between the cooling water and the

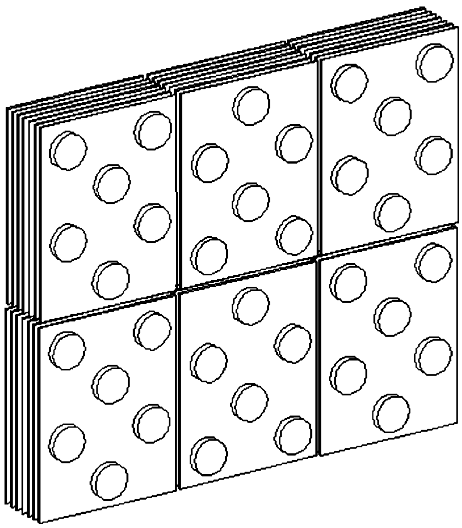

Fig. 1 Schematic diagram of multistage fin-and-tube heat exchanger

inner tube wall, and also the high thermal conductivity of the tube wall, the tube is assumed to be of constant temperature. However, the temperature distribution in the fin surface should be calculated, hence, the problem is of conjugated type in that the temperatures both in the fin solid surface and in the fluid are to be determined simultaneously.

Figure 2 shows the details of the plain fin and the slit fin, which have the same global geometry dimensions. The slit fin is selected from the three different slit fins simulated in [15] due to its best comprehensive performance. The strips on the slit fin surface protrude upward and downward alternatively along the flow direction, with more in rear part and less in the front of the fin. The strip is like a bridge, with its left leg and right leg connected to the base sheet, and the strip is parallel to the base sheet, as can be seen in Fig. 2b. For the slotted fin surface studied, the protruded distance from the base sheet is 1.1 mm and the width of the strip is 2 mm. Numerical simulations are conducted for both plain fin and slit fin under the same other conditions. The detailed geometries of the two types of heat exchanger surfaces are presented in Table 1.

3 Mathematical formulation

3.1 Computational domain

In this study, we define that x is the streamwise coordinate, y is the spanwise coordinate and z stands for the fin pitch direction. Because of the symmetric and periodic characteristics of geometry in y and z directions, the cell between two rows of tubes in y direction and two neighboring fin surfaces in z direction is investigated. The computational domain of the slit fin heat exchanger is shown in Fig. 3.

As it is difficult to simulate the multistage heat exchanger directly, we adopt a new method to implement the numerical modeling stage by stage along the flow direction. For first stage, the uniform velocity and temperatures are assigned at the inlet, while for the other stages the inlet conditions are obtained from the outlet of the former stage, as shown in Fig. 3a. The

Fig. 2 Geometry configuration of the plain fin and the slit fin

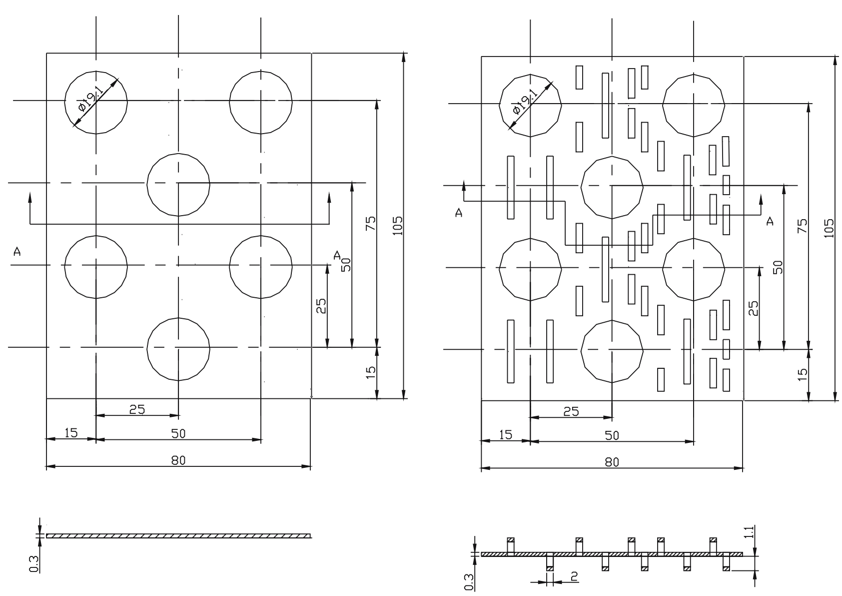

(a) Plain fin **(b)** Slit fin

Table 1 Simulation conditions

Tube outside diameter	19.1 mm
Longitudinal tube pitch	25.0 mm
Transverse tube pitch	25.0 mm
Fin thickness	0.3 mm
Fin pitch	2.5 mm
Strip width	2.0 mm
Strip height	1.25 mm
Tube temperature	35°C
Inlet air temperature	130°C
Inlet frontal velocity	2–10.0 m/s

velocity and temperature distributions in Sect. 1 are obtained from Sect. 2 in the former stage. The numerical simulation can be conducted stage by stage, thus the whole performance of the multistage heat exchanger can be obtained from the numerical results for all individual stages included. This idea can also be extended to many other complex geometries. For the first stage, due to the thickness of the fin, the air velocity profile is not uniform at the entrance, so the computational domain is extended upstream 1.5 times of streamwise fin length, but the computational domains of other stages are not extended in their upstream direction.

Except the last stage, because the fins and tubes in the next stage may exert some influence on this calculated stage, the computational domain is extended to the first tube of the next stage, as shown in Fig. 3a. In order to avoid the recirculation at the computational domain outlet and apply the outflow condition, the computational domains in all the stages are extended downstream ten times of streamwise fin length. For the last stage, although there is no any fin or tube behind it, the computational domain is still extended for the execution of out flow boundary condition as shown in

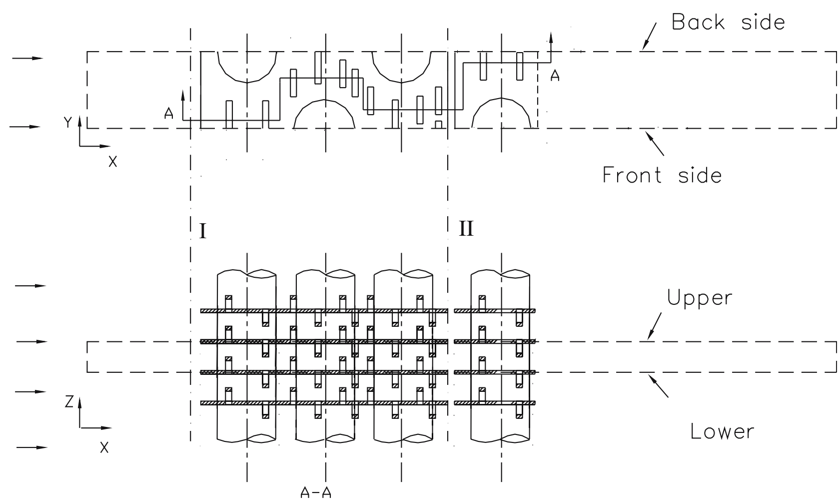

(a) stage with extension

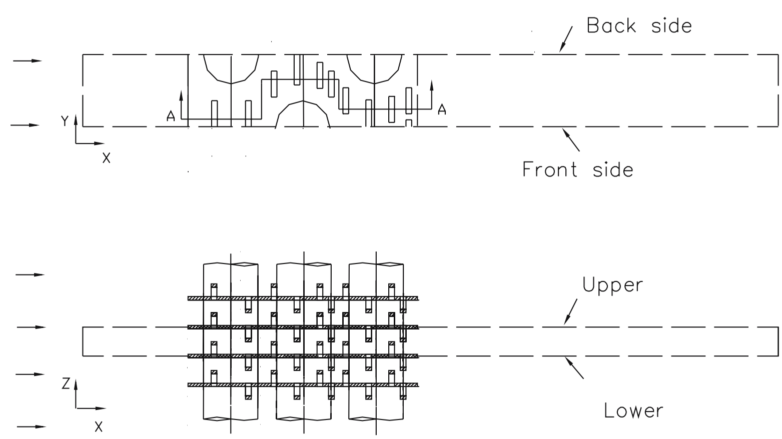

(b) Domain of the last stage

Fig. 3 Computational domain of slit fin

Fig. 3b. For saving space, all the extended domains are not presented in scale in Fig. 3. The dashed lines show schematically such a computational domain in the x–y and z–x planes.

3.2 Governing equations and boundary conditions

The air flow is assumed to be three-dimensional, laminar and steady, then the governing equations for continuity, momentum and energy in the computational domain can be expressed as follows.

Continuity equation:

$$\frac{\partial}{\partial x_i}(\rho u_i) = 0 \tag{1}$$

Momentum equations:

$$\frac{\partial}{\partial x_i}(\rho u_i u_k) = \frac{\partial}{\partial x_i}\left(\mu \frac{\partial u_k}{\partial x_i}\right) - \frac{\partial p}{\partial x_k} \tag{2}$$

Energy equation:

$$\frac{\partial}{\partial x_i}(\rho u_i T) = \frac{\partial}{\partial x_i}\left(\Gamma \frac{\partial T}{\partial x_i}\right) \tag{3}$$

where $\Gamma = \frac{\lambda}{c_p}$

The governing equations are elliptic in the Cartesian coordinate, hence boundary conditions are required for all boundaries of the computational domain. Due to the conjugated type of the problem, the fin surfaces are considered as a part of the solution domain and will be treated as a special type of fluid. The required conditions are described for the three regions as follows:

(1) In the upstream extended region (inlet domain):

at the inlet: for the first stage $u = \text{const}$, $v = w = 0$,

$$T_{\text{in}} = \text{const}; \tag{4a}$$

for the other stages u,v,w,T get from the former stage

at the upper and lower boundaries: $\frac{\partial u}{\partial z} = \frac{\partial v}{\partial z} = 0$,

$$w = 0; \quad \frac{\partial T}{\partial z} = 0 \tag{4b}$$

at the front and back sides: $\frac{\partial u}{\partial y} = \frac{\partial w}{\partial y} = 0, \quad v = 0;$

$$\frac{\partial T}{\partial y} = 0 \tag{4c}$$

(2) In the downstream extended region (outlet domain):

at the upper and lower boundaries: $\frac{\partial u}{\partial z} = \frac{\partial v}{\partial z} = 0$,

$$w = 0; \quad \frac{\partial T}{\partial z} = 0 \tag{5a}$$

at the front and back sides: $\frac{\partial u}{\partial y} = \frac{\partial w}{\partial y} = 0, \quad v = 0,$

$$\frac{\partial T}{\partial y} = 0 \tag{5b}$$

at the outlet boundary:

$$\frac{\partial u}{\partial x} = \frac{\partial v}{\partial x} = \frac{\partial w}{\partial x} = \frac{\partial T}{\partial x} = 0 \tag{5c}$$

(3) In the fin coil region

(a) for plain plate fin:

at the upper and lower surfaces $u = v = w = 0$,

$$\frac{\partial T}{\partial z} = 0 \tag{6a}$$

at the front and back sides: fluid region

$$\frac{\partial u}{\partial y} = \frac{\partial w}{\partial y} = 0, \quad v = 0 \tag{6b}$$

fin surface region $u = v = w = 0$ (6c)

tube region $u = v = w = 0, \quad T_{\mathrm{w}} = const$ (6d)

temperature condition for both fin and fluid regions

$$\frac{\partial T}{\partial y} = 0 \tag{6e}$$

(b) for the strip fin: at the upper and lower surfaces:

velocity at solid $u = v = w = 0$ (7)

velocity of the fluid in the slit: periodic conditions
temperature for both solid and fluid: periodic conditions
The other conditions of the strip fin surface are the same as the plain plate fin.

3.3 Numerical methods

The governing equations are discretized by the finite volume method; the convection term is discretized by SGSD scheme [16], and the coupling of pressure and velocity is implemented by CLEAR algorithm [17, 18]. The fluid–solid conjugated heat transfer problem is solved by full-field computation method. The solid in computational domain is regarded as a special fluid with an infinite viscosity. To guarantee the continuity of the flux rate at the interface, the thermal conductivity of fin and fluid adopts individual value, while the heat capacity of solid takes the value of the fluid [19]. To simulate the strip configuration, a special array called LAG is introduced to identify different regions: fluid, fin and tube. The detailed computational method of conjugated heat transfer can be found in references [19–21]. The circular geometry of the tube is approximated by the stepwise method. A very large value of the thermal conductivity is assigned to the tube region to guarantee the tube temperature to be constant. The computational domain is discretized by non-uniform grids, with the fine grids in fin coils region and coarse grids in the extension domain. The total grid points for a single fin in the last stage are $211 \times 85 \times 24$, and those in the other stages are $271 \times 85 \times 24$. The convergence criterion for the velocities is that the maximummass residual of the cells divided by the inlet mass flux is less than 5.0×10^{-6}, and the criterion for temperature is that difference between the two overall heat flux in the successive iterations is less than 1.0×10^{-6}.

When the numerical simulation for the multistage heat exchangers is conducted stage by stage, the inlet temperature is 130°C for both the plain fin heat exchanger and the slit fin heat exchanger. All the stages have the identical mass flux, and in a particular stage the physical property is assumed to be constant, while it may vary in different stages due to temperature variation. The thermophysical properties are obtained from the mean value of the outlet and the inlet temperatures, so an iterative method is needed. Due to the numerical errors during computation, when the governing equations are convergent, the difference of the mass flux between the outlet and inlet in every stage is set to be less than 1%.

4 Results and discussion

4.1 Parameter definitions

Some parameters are defined as follows:

$$Re = \frac{\rho u_m D_e}{\mu} \tag{8}$$

$$Nu = \frac{h D_e}{\lambda} \tag{9}$$

$$h = \frac{Q}{A \Delta T} \tag{10}$$

$$Q = \dot{m} c_P (T_{\text{in}} - T_{\text{out}}) \tag{11}$$

$$\Delta P = P_{\text{in}} - P_{\text{out}} \tag{12}$$

$$f = \frac{\Delta P}{\frac{1}{2}\rho u_m^2} \cdot \frac{D_e}{L} \tag{13}$$

$$\Delta T = \frac{T_{\max} - T_{\min}}{\log\left(T_{\max}/T_{\min}\right)} \tag{14}$$

$$\theta = \arccos\left(\frac{\vec{U} \cdot \nabla T}{\left|\vec{U}\right| |\nabla T|}\right) \tag{15}$$

$$\overline{\theta} = \frac{\iiint\limits_V \theta dv}{\iiint\limits_V dv} \tag{16}$$

where u_m is the mean velocity of the minimum transverse area, D_e is the outer tube diameter, T_{in}, T_{out} are the bulk temperature of inlet and outlet of the fin surface, respectively, $T_{\max} = \max(T_{\text{in}} - T, T_{\text{out}} - T_{\text{w}})$, $T_{\min} = \min(T_{\text{in}} - T_{\text{w}}, T_{\text{out}} - T)$. It should also be noted that the air-side heat transfer coefficient h has included the surface efficiency.

4.2 Comparison between computational and experimental results

To validate the computational model and the method adopted in numerical simulation for the multistage heat exchanger, preliminary computations were first conducted for the three-row slit fin heat exchanger. The corresponding experiment was also carried out which covers the velocity range in the computation. A schematic diagram of the test apparatus is presented in Fig. 4. It is made up of two loops, an air loop and a vapor loop. The air loop is operated in a suction mode. Air from the room passes through an entrance, a rectifier section, a contract section and a stabilizer before reaching the test section. The test section is an air–vapor heat exchanger in which air is going through the fin surfaces studied and vapor is condensing inside vertical tubes. The heated air leaving the test section passes through a flow metering duct before being discharged to the outdoor by a blower. The steam vapor is generated in electrically heated boiler. The generated vapor is slightly overheated to ensure that at the test section vapor inlet there is no any water drops. The condensate goes to a volumetric flow meter and then return to the boiler. The air temperature difference

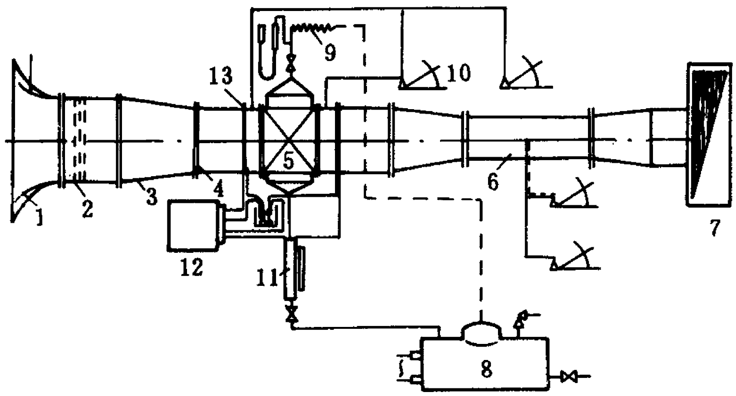

Fig. 4 Schematic diagram of the test section

1. inlet 2. rectifier 3. contract section 4. steady section 5. test section 6. flow rate measurement section 7. blower 8. boiler 9. vapor super-heater 10. inclined manometer 11. volumetric flow rate 12. digital voltmeter 13. thermocouple grids

before and after the test section are measured by two sets of multi-junction copper-constantan thermocouple grids. Each set has 16 grid points, whose junctions are interconnected in series to give a single reading. The air flow rate is measured by a Pitot-tube situated in the flow rate measuring duct far downstream of the test section. The average static pressure before and after the test section are also measured by the inclined manometers. The heat balance between the air-side and the condensate is controlled less than 5%. From the overall heat transfer coefficient measured the air-side average heat transfer coefficients are obtained by subtraction the thermal resistance of the vapor condensation and tube wall heat conduction from the total thermal resistance.

The comparison of numerical and experimental results are provided in Fig. 5, from which we can see that the computational results for pressure drop agree well with the tested data, and the maximum deviation is less than 12%. At the most range of velocity variation, the predicted Nusselt number agrees quite well with the experiment results, and the maximum deviation occurs when the inlet velocity is 2 m/s, which is about 28%. For such a complex multistage slit fin heat exchanger this deviation is acceptable. This comparison proves the reliability of the physical model and code developed.

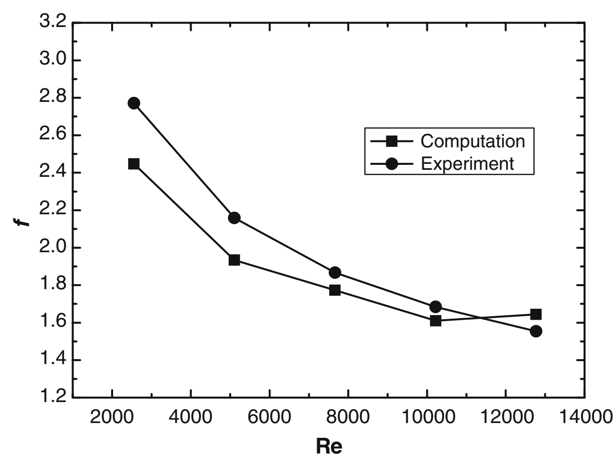

(a) Pressure drop Δp

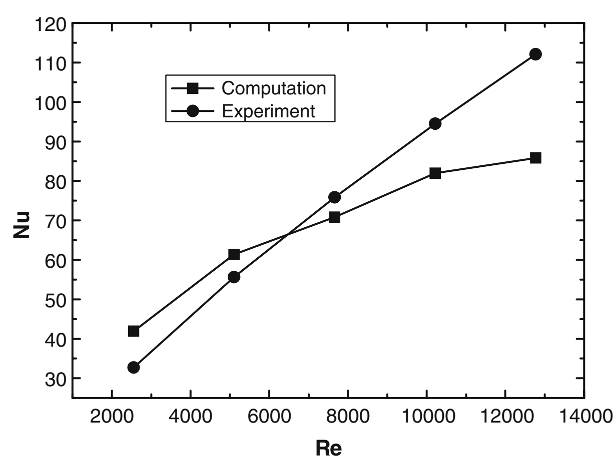

(b) Nusselt Number

Fig. 5 Comparison between predicted and test results for slit fin heat exchanger

4.3 Comparison of the performance of the whole heat exchanger

When three-stage heat exchanger is simulated stage by stage at a certain inlet velocity, the overall heat transfer rate and pressure drop can be obtained through the values from the individual stage. In Fig. 6,

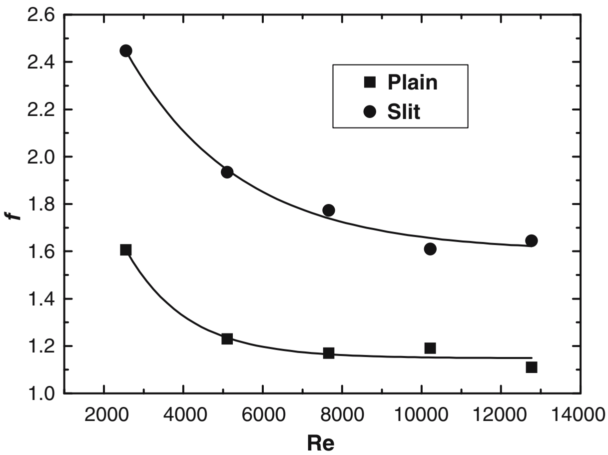

(a) Friction factor

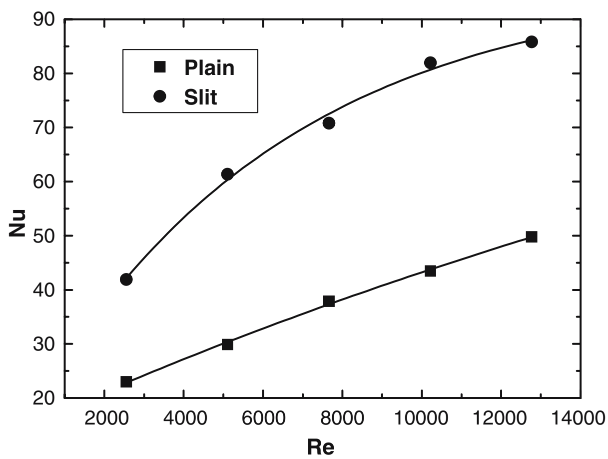

(b) Nusselt number

Fig. 6 Comparison between plain fin and slit fin multistage heat exchanger

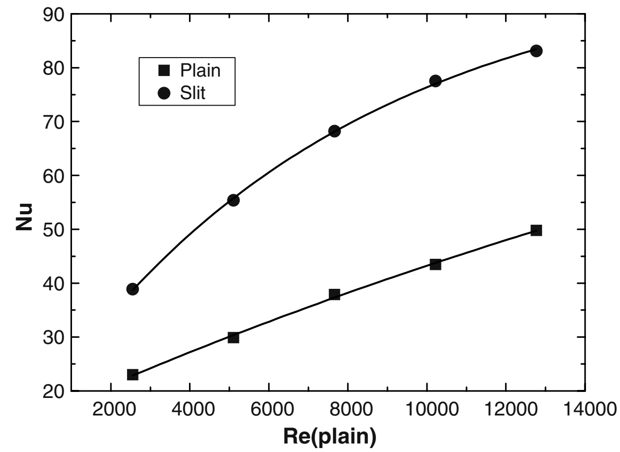

Fig. 7 Performance comparison at the identical pumping power

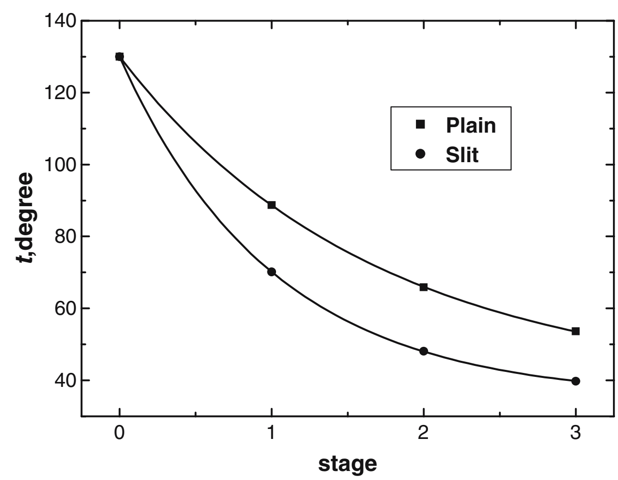

Fig. 8 Temperature variation against stage

the whole pressure drop and average Nusselt number of the multistage heat exchanger are shown. Due to the existence of strips on the fin surface, the whole pressure drop and average Nusselt number in the slit fin heat exchanger are higher than those in the plain fin heat exchanger. However, there is only an average 50% increase in the pressure drop, while the increase in Nusselt number is 87%, which means that under the same pressure drop there will be more heat transfer rate in the slit fin heat exchanger than that in the plain fin heat exchanger. This indicates the excellent comprehensive performance of the slit fin heat exchanger. Figure 6 actually presents the comparison between plain fin and the slit fin at the identical flow rate. A more meaningful comparison is conducted at the constraint of identical pumping power. As derived in [22], for the cases studied, the constraint of identical pumping power leads to following requirement:

$$(f\mathrm{Re}^3)_{\mathrm{plain}} = (f\mathrm{Re}^3)_{\mathrm{slit}} \tag{17}$$

This condition implies that for the same pumping power the frontal velocity of slit fin should be less than that of plain fin because of the increased friction factor of the slit fin. From the exnumerical data and the fitted curve, several pairs of corresponding Reynolds number can be found iteratively each of whom has the same pumping power. Then from the Reynolds numbers corresponding Nusselt numbers can be determined. The ratio of such two Nusselt numbers is presented in Fig. 7, where the abscissa is the Reynolds number of the plain fin. Within the variation range of Reynolds number, the Nusselt number of slit fin heat exchanger can be 67 to 85% higher than that of plain fin heat exchanger at the constraint of identical pumping power, which again proves the excellent performance of slit fin heat exchanger.

4.4 Comparison on the performance along the stages

Figure 8 shows the temperature changes along the stages in two heat exchangers when the inlet velocity is 8 m/s. Due to the heat transfer enhancement in the slit fin heat exchanger, the temperature in it decreases more quickly than that in the plain fin heat exchanger. However, because of the deceasing temperature difference between the incoming air and the wall, the overall heat flux in every stage is also decreasing, so temperatures change more and more mildly along the stages. The outlet temperature in the slit fin heat exchanger is about 40°C while in the plain fin heat exchanger it is about 54°C, which means that it will need more stages to allow the outlet temperature below 40°C.

As expected, the pressure drop in the slit fin heat exchanger increases more quickly along the stages than that in the plain fin heat exchanger, which can be seen in Fig. 9. When the temperature drops along the stages, the air density increase a little, but because the mass flux is constant, the average velocity will definitely deceases, as shown in Fig. 10. Due to the larger temperature variation along the stages in the slit fin heat exchanger, the average velocity in it decreases more quickly than that in the plain fin heat exchanger. As the pressure drop is greatly influenced by the inlet velocity, the pressure drop will be reduced with the decreasing velocity; therefore along the stages the increase of overall pressure drop becomes mild, which is more obvious in slit fin heat exchanger.

Figure 11 shows the Nusselt number variation along the stages when the inlet velocity is 8 m/s. It is apparent that the Nusselt number in the slit fin heat exchanger is much higher than that in the plain fin heat. Take the first stage as example, the Nusselt number in the slit fin heat exchanger can be 83% higher than that in the plain fin heat exchanger. According to the conventional understanding, the heat transfer in the former stage should be better than that in the latter stage. However, due to great changes in fluid property along the stages, the Nusselt number in all the stages of the plain fin heat exchanger is almost constant, while in the slit fin heat exchanger the Nusselt number in the latter stage is even higher that in the former stage.

From Fig. 12, we can see clearly the friction factor variation along the stages when the inlet velocity is 8 m/s. Because of the disturbance of the strips in the slit fin, there is a great friction increase in the slit fin heat exchanger compared to the plain fin heat exchanger. The increase ranges from 39 to 47% along the stages, much lower than that in Nusselt number, which shows again the excellent performance of the slit fin in

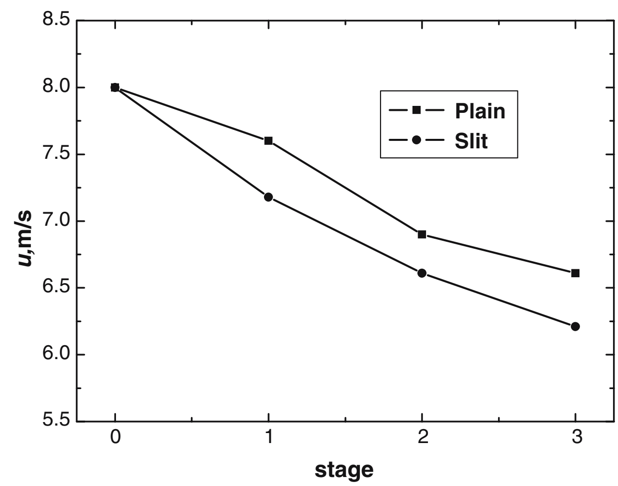

Fig. 10 Averaged inlet velocity against stage

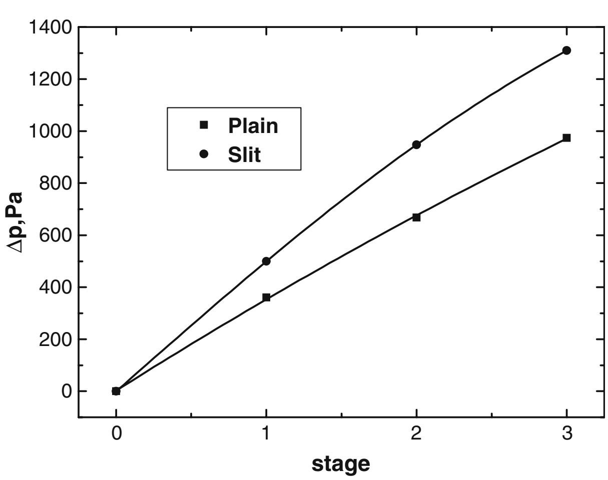

Fig. 9 Pressure drop against stage

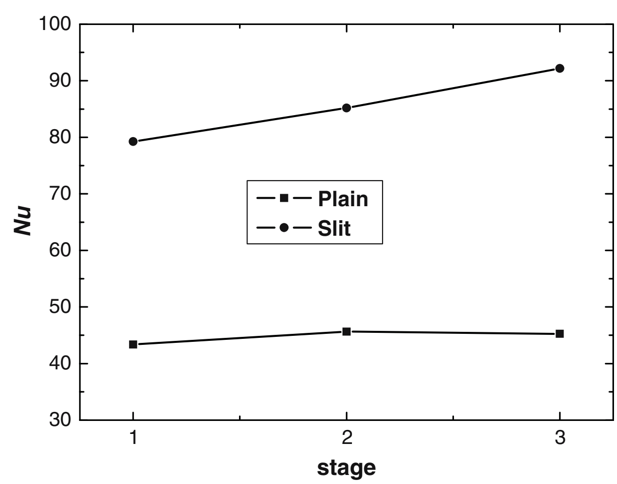

Fig. 11 Nusselt number against stage

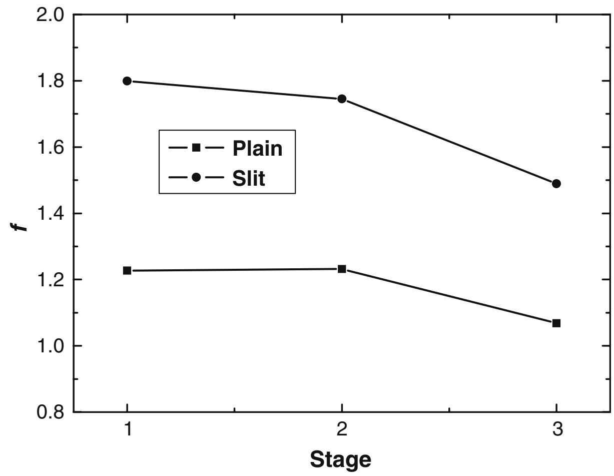

Fig. 12 Friction factor against stage

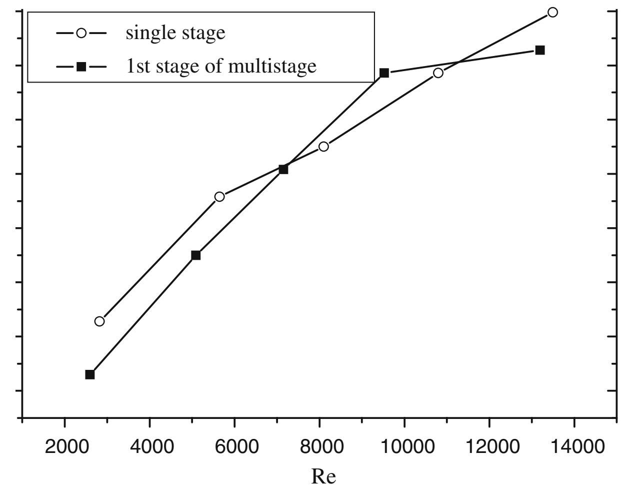

Fig. 13 Comparison of Nu between first stage in multistage and single stage

the multistage heat exchanger. It is interesting to note that the friction factor in the last stage is much less than that in the former stage, which may be caused by the disappearance of the influence of the latter stage, the air can flow out of the heat exchanger with less retardation.

It may be interested to note that the geometrical dimensions of the slit fins in present work are totally identical with those in [15], including the number and position of the slits. However, along the flow direction in [15] there is only a single fin while in the present work there are three aligned fins. Thus the flow in every stage is influenced by that in neighboring stage. However, the first stage of the multistage situation may be comparable with the single stage case because only the exit condition has some difference. Thus comparison is made between the average heat transfer of the first stage in the multistage case and the heat transfer of the single stage. The results are presented in Fig. 13. It can be seen that within the velocity range studied the difference between the two situations is not very significant. This implies that the outflow boundary condition does not have significant effect on the average heat transfer character because of its limited influencing region.

5 Discussion on heat transfer enhancement

From traditional viewpoint, the reason why the slit fin can enhance heat transfer can be attributed to that the strips can interrupt the flow boundary layer to reduce the thermal boundary layer thickness by repeatedly recreation of the thermal boundary layer, or can increase the disturbance in the flow field. Figures 14 and 15 are the velocity field and temperature field in the first stage of the plain fin heat exchanger and slit fin heat exchanger respectively, when the inlet velocity is 8 m/s, which are obtained from the center section in the z direction. From Fig. 11 we can see that most of the air flows in the middle of the flow channel, therefore, only the front and the top of tubes can have sufficient contact with the flow. Due to the vortex behind the tubes, the heat transfer there becomes worse. Except the region near the fin, most of the heat transfer happens in the front and top part of the tubes. When the strips are arranged on the fin surface they can disturb the air greatly between two adjacent fins, as seen in Fig. 12a. The velocity distribution is more uniform in the spanwise direction, and more air will be squeezed toward the back of the tubes, hence more tube surface is involved in heat transfer from the fluid to the tube, which can be seen more apparently from the front two tubes. Furthermore, because the strips protrude into the air, many heat sinks are arranged in the air, which also enhances the heat transfer.

The heat transfer enhancement can also be explained from the viewpoint of field synergy principle proposed by Guo et al. [11, 12]. The main idea is that all the measures for enhancing heat transfer can be attributed to increase the synergy between the velocity and temperature gradient. From Fig. 14 we can see that in most regions of the slit fin, the velocity vector is almost normal to the temperature gradient, which means worse synergy between the velocity field and temperature field. However, in the slit fins, due to the existence of the strips, the velocity and temperature distribution are greatly changed, and the synergy between the velocity and temperature gradient becomes

Fig. 14 Velocity vector and temperature contours of the center section in the *z* direction for plain fin

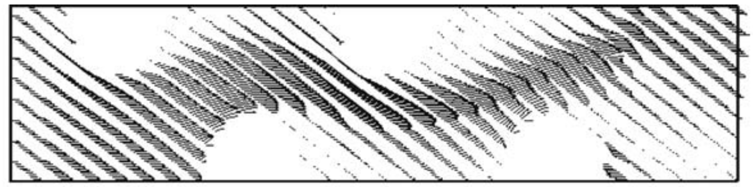

(a) Flow field

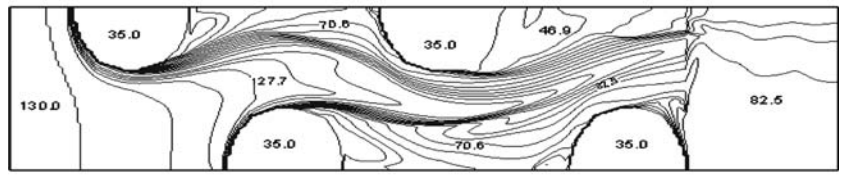

(b) Temperature field

Fig. 15 Velocity vector and temperature contours of the center section in the *z* direction for slit fin

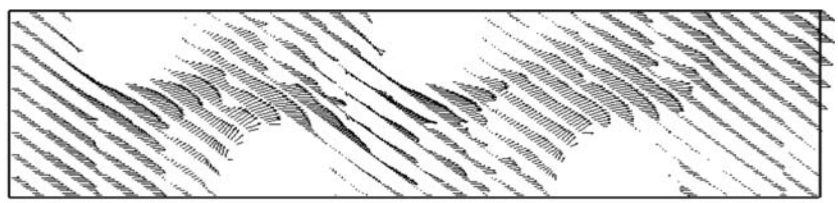

(a) Flow field

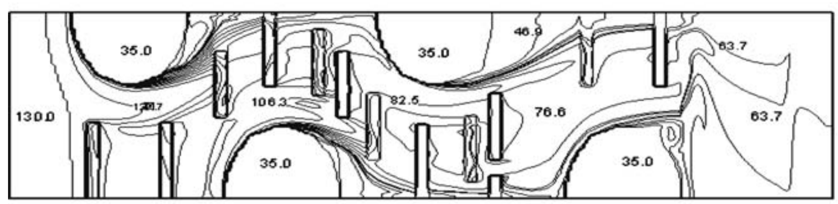

(b) Temperature field

better. Here we use the domain averaged intersection angle (i.e. synergy angle) between the velocity vector and temperature gradient, which is defined in Eqs. 15 and 16. The larger the synergy angle, the worse the synergy between the velocity and temperature gradient. From Fig. 16 we can see that in the three stages, the synergy angle in the plain fin heat exchanger is always higher than that in the slit fin heat exchanger. Because large velocity can deteriorate the synergy between the velocity vector and temperature gradient, the synergy angle in the first stages of the plain fin heat exchanger is higher than that in the following stages. Although the absolute difference of the synergy angle for the second stages is less than 0.4 °, this will lead to the difference in cosine nearly 10%, thus we can conclude that the function of strips on the slotted fin surface is to improve the synergy between the velocity and temperature gradient.

6 Conclusions

In this paper, the air-side heat transfer and pressure drop of two three-stage heat exchangers with plain fin and slit fin is numerically investigated using a three-dimensional steady laminar model, the performance of the two heat exchangers are compared on the whole and along the stages respectively, the results are also analyzed with the field synergy principle. The major findings are summarized as follows:

1. A new method is proposed to simulate the multistage heat exchanger; the comparison between the predicted results and the tested data shows this method is reliable.
2. The performance of the two multistage heat exchangers with plain fin and slit fin is compared, which shows that, compared to the plain fin heat exchanger the slit fin heat exchanger can have an

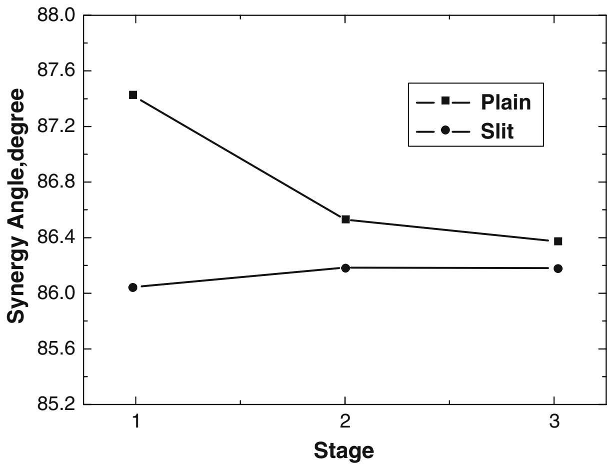

Fig. 16 Domain averaged synergy angle against stage

average 87% higher Nusselt number, while only average 50% higher pressure drop, similar results can also be achieved through the comparison along stages for two kinds of heat exchangers, which shows the excellent performance of the slit fin.

3. The heat transfer enhancement in the slit fin heat exchanger can be attributed to better the synergy between the velocity and temperature gradient.

Acknowledgments This work was supported by the National Natural Science Foundation of China (Grant number 50476046) and the National Key Project of Fundamental R & D of China (Grant No. 2007CB206902).

References

1. Kang HJ, Li W, Li HJ, Xin RC, Tao WQ (1994) Experimental study on heat transfer and pressure drop characteristics of four types of plate fin-and-tube heat exchanger surfaces. Int J Therm Fluid Sci 3(1):34–42
2. Yun JY, Lee KS (1999) Investigation of heat transfer characteristics on various kinds of fin-and-tube heat exchangers with interrupted surfaces. Int J Heat Mass Transf 42:2375–2385
3. Nakayama W, Xu LP (1983) Enhanced fins for air-cooled heat exchangers-heat transfer and friction factor corrections. In: Proceedings of the 1983 ASME-JSME thermal engineering conference, vol 1, pp 495–502
4. Hiroaki K, Shinichi I, Osamu A, Osao K (1989) High-efficiency heat exchanger. Natl Tech Rep 35(6):653–661
5. Wang CC, Tao WH, Chang CJ (1999) An investigation of the air side performance of the slit fin-and-tube heat exchangers. Int J Refrig 22:595–603
6. Du YJ, Wang CC (2000) An experimental study of the air-side performance of the superslit fin-and-tube heat exchangers. Int J Heat Mass Transf 43:4475–4482
7. Wang CC, Lee WS, Sheu WJ (2001) A comparative study of compact enhanced fin-and-tube heat exchangers. Int J Heat Mass Transf 44:3565–3573
8. Yun JY, Lee KS (2000) Influence of design parameters on the heat transfer and flow friction characteristics of the heat exchanger with slit fins. Int J Heat Mass Transf 43:2529–2539
9. Kang HC, Kim MH (1998) Effect of strip location on the air-side pressure drop and heat transfer in strip fin-and-tube heat exchanger. Int J Refrig 22:302–312
10. Qu ZG, Tao WQ, He YL (2004) 3D numerical simulation on laminar heat transfer and fluid flow characteristics of strip fin surface with X-arrangement of strips. ASME J Heat Transf 126:697–707
11. Guo ZY, Li DY, Wang BX (1998) A novel concept for convective heat transfer enhancement. Int J Heat Mass Transf 41:2221–2225
12. Wang S, Li ZX, Guo ZY (1998) Novel concept and devices of heat transfer augmentation. In: Proceedings of 11th international conference of heat transfer, vol 5. Taylor & Francis, London, pp 405–408
13. Tao WQ, Guo ZY, Wang BX (2002) Field synergy principle for enhancing convective heat transfer: its extension and numerical verifications. Int J Heat Mass Transf 45:3849–3856
14. Tao WQ, He YL, Wang QW, Qu ZG, Song FQ (2002) A unified analysis on enhancing convective heat transfer with field synergy principle. Int J Heat Mass Transf 45:4871–4879
15. Cheng YP, Qu ZG, Tao WQ, He YL (2004) Numerical design of efficient slotted fin surface based on the field synergy principle. Numer Heat Transf A 45:517–538
16. Li ZY, Tao WQ (2002) A new stability-guaranteed second-order difference scheme. Numer Heat Transf B Fundam 42(4):349–365
17. Tao WQ, Qu ZG, He YL (2004) A novel segregated algorithm for incompressible fluid flow and heat transfer problems: CLEAR (coupled & linked equations algorithm revised) Part I: mathematical formulation and solution procedure. Numerical Heat Transf B 45:1–17
18. Tao WQ, Qu ZG, He YL (2004) A novel segregated algorithm for incompressible fluid flow and heat transfer problems: CLEAR (coupled & linked equations algorithm revised): Part II: Application examples. Numerical Heat Transfer B 45:19–48
19. Tao WQ (2001) Numerical heat transfer, 2nd edn. Xi'an Jiaotong University Press, Xi'an
20. Patankar SV (1980) Numerical heat transfer and fluid flow. McGraw-Hill, New York
21. Tao WQ (2000) Recent advances in computational heat transfer. Science Press, Beijing
22. Huang HZ, Tao WQ (1993) An experimental study on heat mass transfer and pressure drop characteristics for arrays of non-uniform plate length positioned obliquely to the flow direction. ASME J Heat Transf 115(3):568–575